ARTICLE

Check for updates

Single-cell transcriptional profiling of murine conjunctival immune cells reveals distinct populations expressing homeostatic and regulatory genes

Jehan Alam[1], Ghasem Yazdanpanah[1], Rinki Ratnapriya[1], Nicholas Borcherding[2], Cintia S. de Paiva[1], DeQuan Li[1] and Stephen C. Pflugfelder[1]✉

Immune cells in the exposed conjunctiva mucosa defend against environmental and microbial stresses. Expression profiling by single-cell RNA sequencing was performed to identify conjunctival immune cell populations expressing homeostatic and regulatory genes. Fourteen distinct clusters were identified, including myeloid cells (neutrophils, monocytes, macrophages), dendritic cells (DC), and lymphoid cells (B, T, γδT, ILC2, and NK) lineages. Novel neutrophil [lipocalin (*Lcn2*) high and low), and MHCII[lo] macrophage (MP) clusters were identified. More than half of the cells map to myeloid and dendritic cell populations with differential expression profiles that include genes with homeostatic and regulatory functions: *Serpinb2* (MHCII[lo] macrophage), *Apoe* (monocyte), *Cd209a* (macrophage), *Cst3* (cDC1), and *IL4i1* in migratory DC (*mDC*). ILC2 expresses the goblet cell trophic factor IL-13. Suppressed inflammatory and activated anti-inflammatory/regulatory pathways were observed in certain myeloid and DC populations. Confocal immunolocalization of identity markers showed mDC (CCR7, FASCIN1) located on or within the conjunctival epithelium. Monocyte, macrophage, cDC1 and IL-13/IL-5^{+} ILC2 were located below the conjunctival epithelium and goblet cells. This study found distinct immune cell populations in the conjunctiva and identified cells expressing genes with known homeostatic and immunoregulatory functions.

INTRODUCTION
The conjunctiva is a unique mucosal tissue that is exposed to the environment, produces, and secretes tear-stabilizing goblet cell mucins, and provides immune surveillance for the clear avascular cornea. A variety of immune cells including, myeloid, dendritic, natural killer (NK), B cells, and conventional and unconventional T cells, have been identified in the conjunctiva by immunostaining or flow cytometry using antibodies to conventional lineage markers[1–4]. Certain antigen lineage markers are recognized to lack specificity. For example, the integrin CD11b is expressed by a variety of cells, including neutrophils, eosinophils, monocytes, macrophages, dendritic cells, and NK cells[5].

Because the conjunctival immune system is subjected to danger signals from bacterial, fungal, parasitic, and viral pathogens, as well as desiccating and osmotic stress, regulation of the immune response is of paramount importance to prevent loss of conjunctival goblet cells and exuberant sight-threatening corneal inflammation and proteolysis[6,7]. Certain cytokines and pathways have been found to have homeostatic functions in the conjunctiva. The cytokine IL-13 was found to be a trophic factor for the conjunctival goblet cells[8,9]. Retinoids, secreted into tears and produced by the conjunctival goblet cells suppress the production of inflammatory mediators[10]. Nevertheless, there is much to discover regarding which conjunctival cell populations produce homeostatic and regulatory factors and how these cells interact.

This study used single-cell transcriptional profiling of murine conjunctival immune cells to identify distinct populations expressing homeostatic and regulatory genes and specific identity markers based on gene expression profiles.

RESULTS

Single-cell transcriptome profiles reveal heterogeneous immune cell populations in the C57B/6 mouse conjunctiva
We performed droplet-based single-cell RNA sequencing (scRNA-seq) as an unbiased approach to evaluate immune cell types in the mouse conjunctiva. We constructed a scRNA-seq library from CD45^{+} immune cells sorted from the conjunctiva of normal C57BL/6 J (B6) mice ($n = 8$ biological replicates) and obtained a transcriptomic profile of 11,165 cells using the x10 Genomics platform (Fig.1a). The scRNA-seq data analysis was performed using Seurat V4.1.0. After quality assessment (Fig. S1a), filtering standard pre-processing, and doublet exclusion (Fig. S1a), a total of 8909 cells with 2500 variable features were analyzed. Graph-based clustering using Seurat divided the cells into 14 clusters (Fig. 1b) that were identified based on the expression of signature marker genes listed in Table S1. The identified clusters include

[1]Department of Ophthalmology, Baylor College of Medicine, Houston, TX, USA. [2]Department of Pathology, Washington University School of Medicine, St. Louis, MO, USA.
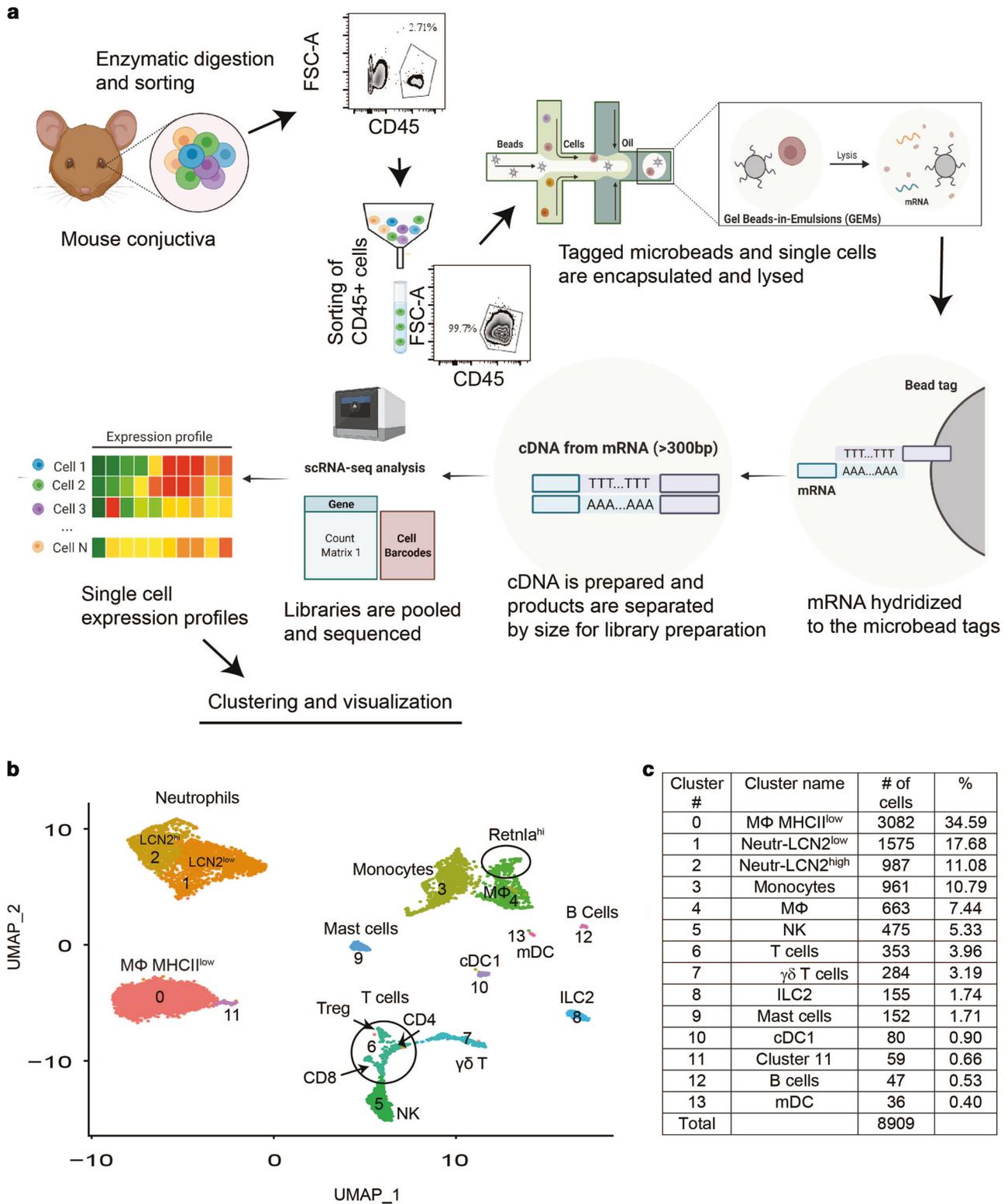✉email: stevenp@bcm.edu

Fig. 1 Summary of scRNA-seq methods and scRNA-seq reveals heterogeneous cell populations in the conjunctiva of B6 normal mice. a Flow diagram of experimental protocol for scRNA-seq library construction and analysis. **b** UMAP of conjunctival immune cells generated from single-cell transcriptomic profiles of 8909 total cells obtained from 8 mice female C57BL/6 J identifies 14 cell clusters using Seurat package v4.1.0. **c** The cell count and percentage for clusters is shown in the table.

neutrophil, monocyte, macrophage, mast cell, natural killer cell, T cell, group 2 innate lymphoid cells (ILC-2), γδ-T cell, B cell, conventional dendritic cells 1 cDC1 and migratory dendritic cell (mDC) lineages (Fig. 1b). The number of cells and percentage of

the whole population in each cluster are shown in Fig. 1c. Myeloid cells (monocytes and macrophages) in clusters 0, 3, and 4 comprise approximately half (52.82%) of the total cells. Cluster 0 contains the largest percentage of cells (34.59%) that express both

macrophage, granulocyte and eosinophil-associated genes. This cluster is identified as macrophage MHCII[lo] because it expresses class 2 antigens and eosinophils were not visualized in tissue sections by histochemical (H&E or congo-red) staining. UMAP features plots of highly expressed genes in Fig. S1b show their cluster specificity. Cluster 4 has a subpopulation of Retnla^{hi} cells (Fig. S1b, last row, left). Cluster 6 (T cells) contains cells expressing markers for three T cell lineages, including CD8, CD4, and Treg (Fig. S1b, last row, right). A heatmap of the top 10 differentially expressed genes in each cluster is shown in Fig. S2 and Table S2 lists all of the differentially expressed genes. Taken together, our single-cell transcriptomic atlas reveals that the heterogeneous immune cell population in the conjunctiva of B6 mice consists of cells with distinct gene expression profiles.

The gene expression profiles provide insight into the function of certain cell types. Neutrophils are segregated into 2 groups with one having higher expression of lipocalin 2 (Lcn2, a.k.a.Ngal), a molecule involved in innate immunity. Lipocalin 2 prevents degradation of the gelatinase MMP-9 and has been found to increase in tears during sleep, in ocular graft vs. host disease (GVHD), and corneal alkali burn[11–13]. Apoe is the highest expressed gene in the monocyte cluster. Apoe has been found to modulate the uptake of apoptotic cell remnants by phagocytic cells and suppress inflammation[14]. Monocytes also express high levels of M2 macrophage genes, including Chil3 and Mrc1[15]. γδ-T cells (cluster 7) have high Il17 expression. IL17 expression has been found to increase in the conjunctiva/cornea in dry eye and it stimulates proteases that are involved in corneal barrier disruption[16,17]. A subset of macrophages (cluster 4) 4 has high expression of Retnla, a factor induced by retinoic acid and IL-4, and Mrc1 (CD206) a c-type lectin that scavenges unwanted high mannose N-linked glycoproteins found on the surface of microbes, including bacteria, fungus, viruses and parasites[18,19]. The most abundant gene expressed by type 1 conventional dendritic cells (cDC1) is cystatin 3 (Cst3), a factor that inhibits the cysteine protease cathepsin S (CTSS) that has an important function in MHC-class-II-restricted antigen presentation[20]. Cystatin C decreases and CTSS increases in tears of Sjögren syndrome (SS) patients[21]. cDC1 also express the integrin Itgae (CD103) and Toll-like-receptor 3 (Tlr3). The migratory DC cluster has a very similar expression profile to mregDCs that are regulated by IL-4/IL-13, and suppress T cell immunity when they infiltrate tumors[22]. This cluster has high expression of Ccr7, a chemokine receptor that directs DC migration to draining lymphatics, chemokines Ccl17 and Ccl22 that respectively recruit and polarize regulatory T cells[23,24], IL-4 inducible gene 1 (Il4I1), Il4ra1, Fscn1 an actin filament binding protein associated with the development of membrane protrusions and assembly of the immune synapse in DCs and the retinoic acid metabolizing gene Aldh1a2[25]. TLRs were not found among the differentially expressed genes (DEG) in the mDC cluster. IL-4 has been reported to suppress maturation and MHCII expression by DCs and up to 22% of patients treated with anti-IL-4RA for atopic dermatitis have been reported to develop severe conjunctival inflammation[26,27].

Conventional flow cytometry cell surface markers are found on a variety of cells with distinct gene expression profiles
Our lab and others have previously identified heterogeneous conjunctival immune cell populations with flow cytometry or immunostaining using antibodies to conventional cell surface antigens[3–5,28]. scRNA-seq identifies the diverse conjunctival immune cell populations with higher resolution. The sequencing data shows that genes encoding conventional myeloid cell markers, including CD11b, CD11c, and Ccr2 are expressed by several cell types, including non-myeloid cells and lack specificity for any particular cell type (Fig. 2a). In contrast, Fig. 2b demonstrates that many of the markers used to identify the conjunctival cell clusters show high expression levels primarily in that cluster; however, there is overlap for some markers (i.e. Marcksl1, Cd74, H2-Ab1) between myeloid and dendritic cells and Jund transcription factor is expressed by all clusters.

Cell-cell interaction and pathway analysis
To determine communications between the conjunctival immune cells, we uploaded Seurat objects into cellchat to determine the number and strength of ligand-receptor interactions. The aggregate cell-cell communication network is shown by the total number of links (Fig. 3a, left) or the strength of the links between cell types (Fig. 3a, right). We also visualized the dominant cell signals senders and receivers in a 2D space using scatter plot (Fig. S3). Myeloid (monocytes and macrophages) and dendritic cells (cDC1 and mDC) were found to have the strongest interactions with each other.

Detectable genes in each cluster were used for determining the strength of association with canonical pathways using Qiagen IPA (Fig. 3b). In the monocyte, macrophage and cDC1, and populations, inflammatory pathways (interferon, IL-1, and TLR signaling and DC maturation) are inhibited, while regulatory/anti-inflammatory pathways are enriched (PPAR signaling, LXR/RXR activation, PPAR/RXRα activation, PTEN signaling and aryl hydrocarbon receptor signaling). RXRα expression is higher in myeloid cells and Aldh1a2 that is involved in retinoic acid metabolism is higher in macrophage and mDC (Fig. 3c).

Expression and spatial localization of myeloid and dendritic cells markers
Confocal microscopy was used to detect differentially expressed markers in myeloid, DC, and ILC2 clusters that are involved in the maintenance of homeostasis and immune tolerance.Cells staining positivity for these factors along with violin plots showing the cluster-specific expression levels of these factors are shown in Fig. 4. The epithelial (E) stromal (S) junction is marked with a line. Proteins associated with mDC (CCR7 and FASCIN; 30.3 ± 5.1% of CCR7^{+} cells are FSCN1^{+}) are detected in cells located on the conjunctival surface and superficial stroma (Fig. 4a). CST3 positive cDC1 were located below the epithelium (Fig. 4b). Markers associated with monocyte (CSF1R and APOE; 27.3 ± 3.2% of CSF1R^{+} cells are ApoE^{+}, macrophage (CD209a, MHCII; 81 ± 1% of CD209a^{+} cells are MHC-II^{+}), macrophage MHCII^{lo} (SERPIN B2 and ADGRE1-F4/80; 6 ± 6.5% of ADGRE1^{+} cells are SERPINB2^{+}), and ILC2 (IL-5 and IL-13; 84 + 1.4% of IL-5^{+} cells are IL-13^{+}) localized to cells found in the stromal near wheat germ agglutinin (WGA) lectin positive goblet cells (Fig. 4c–f), respectively. Retnla[hi] macrophages shown in Fig. S4a, left reside at the surface of the conjunctiva (RETNLA and MRC1; 61.5 ± 10.6% of MRC1^{+} cells are RETNLA[+]).

MHCII staining was noted in CCR7^{+} mDC on the surface (Fig. S4a, middle) (35.7 ± 4.2% of MHC-II^{+} cells are CCR7^{+})and CST3^{+} positive cells in the superficial stroma of the conjunctiva (Fig. 4bc) (48.5 ± 7.8% of CST-3^{+} cells are MHC-II[+]) CCR7^{+} mDCs were aligned or colocalized with LYVE-1^{+} lymphatic vessels (Fig. S4a, right) (66 ± 15.5% of LYVE-1^{+} cells are CCR7^{+}). Cluster-specific expression of other anti- and pro-inflammatory genes is provided in Figs. S4b and S4c2, respectively.

DISCUSSION
Functions of the conjunctival immune cells include pathogen defense, trophic support of the mucin secreting goblet cells, wound healing, and production of regulatory factors to minimize tissue-damaging inflammation. Characterization of conjunctival immune cells in the past has primarily relied on immunostaining or flow cytometry using antibodies to conventional lineage markers. Immune cells, including monocyte derived macrophages and DCs, macrophages and T cells were were also identified by our study that used scRNA-seq to profile immune cells at a deeper level. To the best of our knowledge, this is the first report using this technology to profile gene expression in conjunctival immune cells. Collin, Queen, Zerti, Bojic, Dorgau, Moyse and colleagues reported single cell transcriptional profiles of cells isolated from the human limbus. Five immune cell types (monocyte derived macrophage/dendritic cells, 2 types of macrophages and
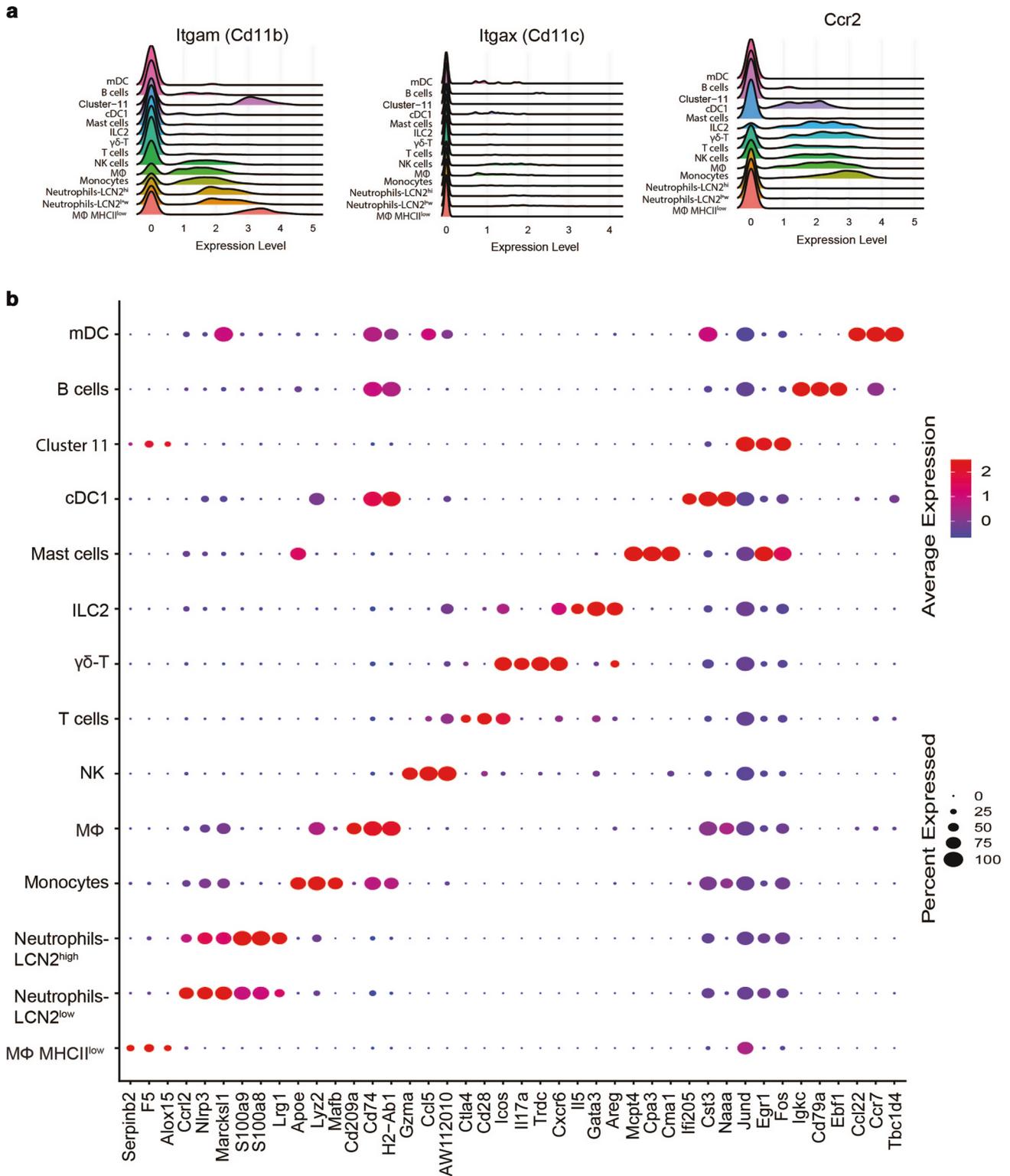
Fig. 2 Conventional cell identity markers and cell identity by sc-RNAseq. a Ridge plots displaying the expression of three conventional immune markers use for flow cytometry by cluster identity. X-axis indicates level of expression level; **b** Dot plot showing top three DEG as alternative markers for each cluster identity. Size of the dot equates to the percent of cells of the cluster expressing the marker. Color of dots based on natural log of the normalized RNA expression.

2 CD8 T cells) were identified. Top differentially expressed genes by these cells aligned with similar cell types we found in the conjunctiva except for the CD81 cluster[29]. We identified 14 cell clusters and most clusters mapped to the cell types with the highest identity match in

the CIPR database. The lowest identity match was for cluster 0 that we designated macrophage MHCII[lo]. *Alox15*, an eosinophil-associated marker, and *Adgre* (F4/80), a gene expressed by macrophages and eosinophils were among the top differentially expressed genes in this
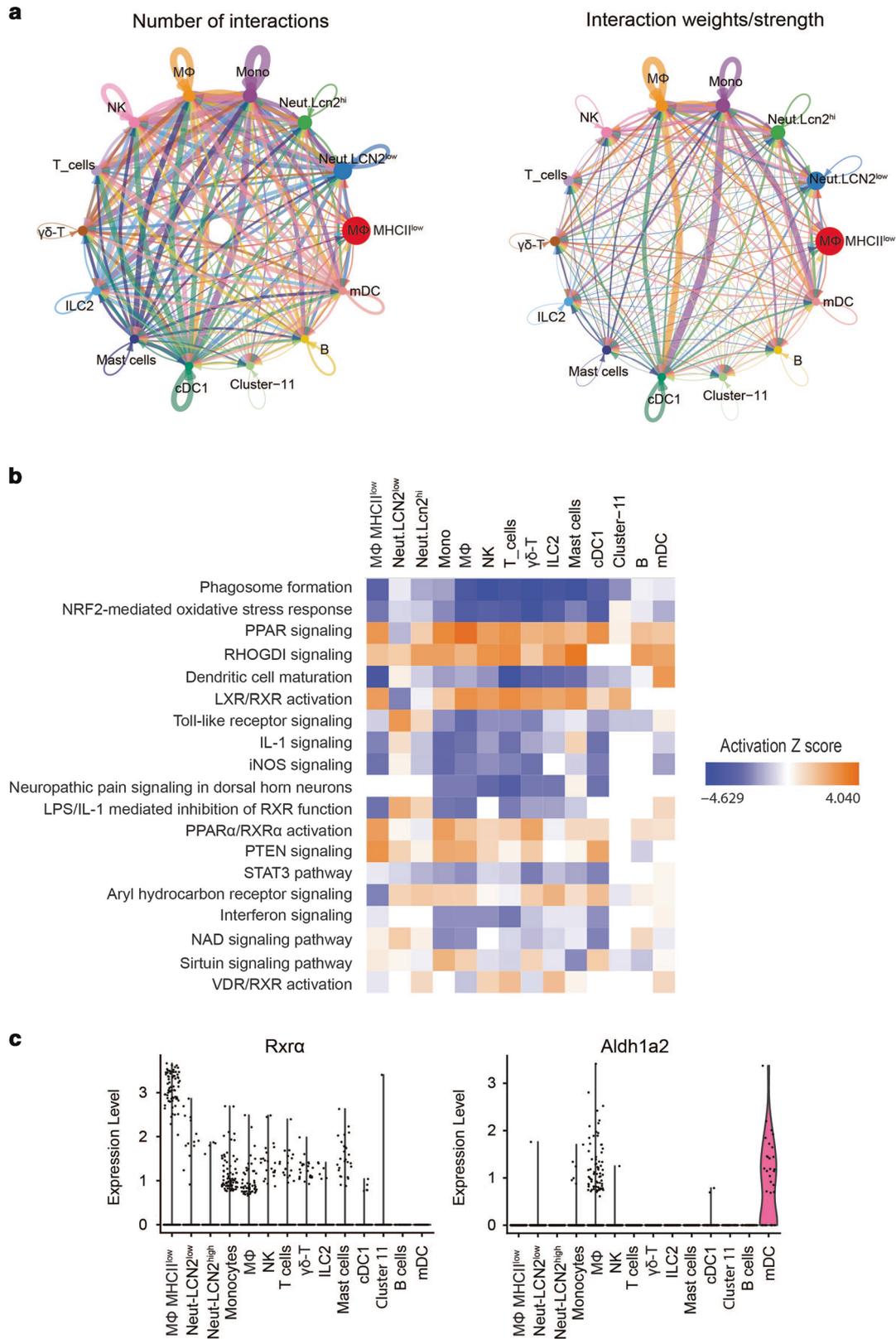
a Number of interactions / Interaction weights/strength

b

c

Fig. 3 **Cell-cell interaction, enriched pathways and expression of retinoid pathway genes. a** Circle network plots showing number (left) and weights/strengths of cell-cell interactions generated with cellchat.; **b** Relative enrichment based on pathway analysis generated with Qiagen IPA, **c** Violin plots of RXRα and *Aldh1a2* expression in cell clusters.
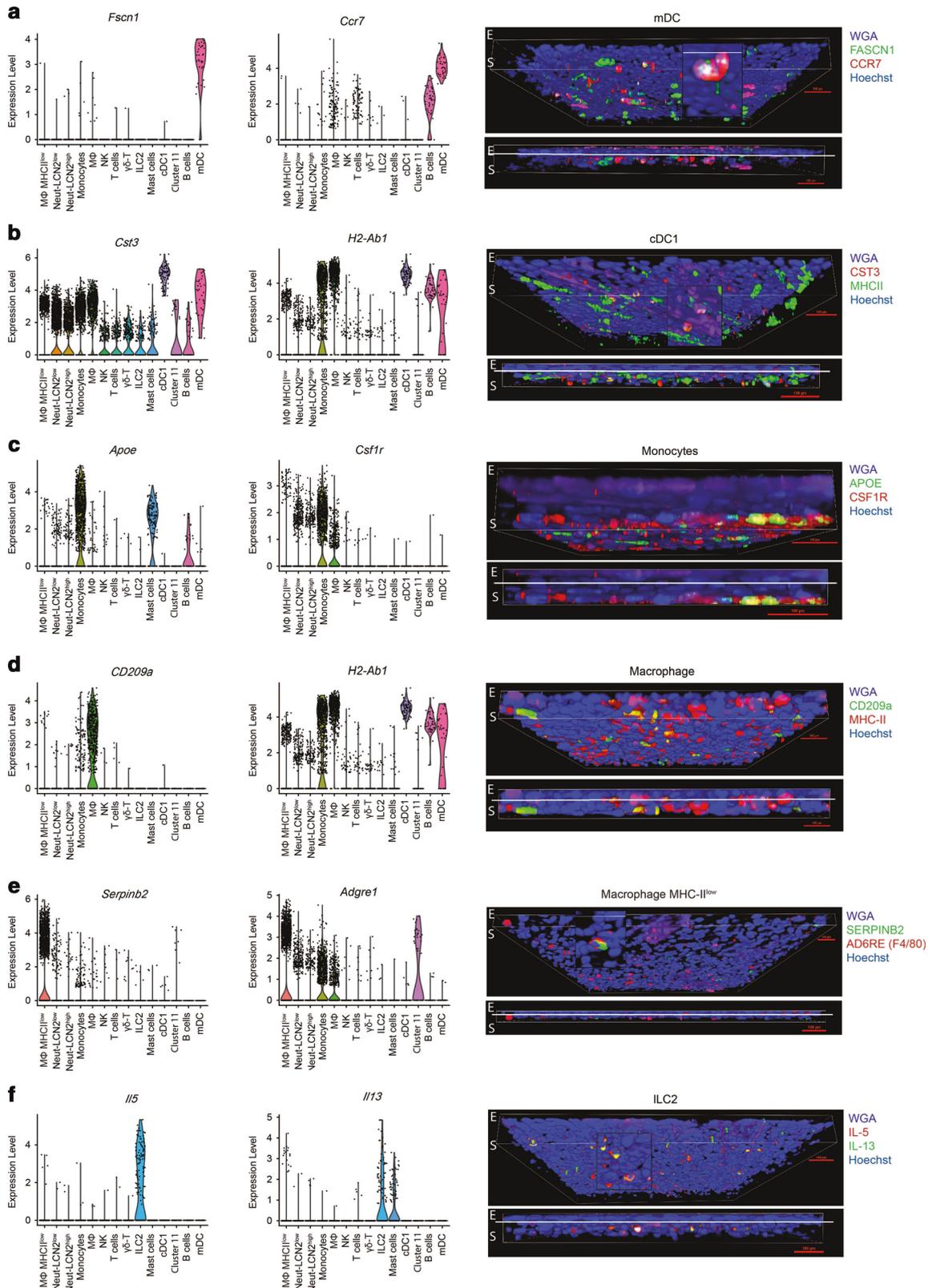
Fig. 4 Cluster specific expression (left) and confocal immunolocalization of cluster-specific factors (in parenthesis) in conjunctival whole mounts. a Ccr7 and Fscn1 (mDC); b MHCII and CST3 (cDC1); c APOE (monocyte) and CSF1R (CD115) (monocytes); d CD209a and MHCII (macrophage); e SERPINB2 and ADGRE (F4/80) (macrophage MHCIII^ow); f IL-13 and IL-5 (ILC2). Scale bar = 100 μm. Biological replicates (n = 3) and technical replicates (n = 2).

cluster; however, eosinophils were not observed by histochemical staining in the conjunctiva. Expression of some traditional cell antigen markers was found in several clusters, indicating their relative lack of specificity. The expression profiles revealed genes, for example, *Serpinb2* (macrophage MHCIIlow), *Apoe* (monocyte), *IL5* for ILC2 and *Fascn1* (mDC), that can be used for cell identification and/or provide insight into the function of these cells.

Mapped clusters include myeloid cells (neutrophil, monocyte, macrophage), two DC clusters (cDC1, mDC), and lymphoid cells (B, T, γδT, ILC2, and NK). Novel lipocalin2 (*Lcn2*) high and low neutrophil, and Retnla[hi] macrophage subclusters were identified. Myeloid and dendritic cells were the predominant populations comprising 54.12 % of the isolated cells. These cells express genes with known homeostatic (protease inhibitors) and regulatory functions (anti-inflammatory and tolerance induction). Among these, *Serpinb2* (macrophage MHCII[lo]), also known as plasminogen activator inhibitor, suppresses activation of plasmin, which in turn can promote ocular surface inflammation by activating complement and metalloproteases and generating fibrin degradation products. *Cst3* (cystatin C) expressed by cDC1 inhibits activation of *CTSS*, a protease involved in MHCII-restricted antigen presentation[20,21]. Reduced levels of CST3 in the tears has been implicated as a cause for the increased tear CTSS activity that is associated with disease severity in Sjögren syndrome associated keratoconjunctivitis sicca[21]. *Apoe* the top differentially expressed gene by the monocyte cluster, has been found to suppress macrophage recruitment and activation, independent of its role in lipid transport[14,30]. It also functions in scavenging apoptotic cell bodies, an activity that also suppresses inflammation[14]. Cd209a (DC-sign), the top differentially expressed gene in the macrophage cluster is associated with the generation of immune tolerance[31]. Expression of IL-4 signature genes (*IL4i1, IL4ra*) in the mDC cluster is characteristic of regulatory DCs that promote immune tolerance and suppress generation of IFN-γ producing T cells[22]. cDC2 has been previously identified in the conjunctiva using cell surface markers[32], but was not identified as a distinct cluster based on a unique transcriptional profile. cDC2 is a heterogenous cell population that shares markers with monocyte derived DCs and macrophages, particularly at inflamed mucosa[33]. It is possible cDC2 is included in macrophage cluster that shows strong correlation (94–100%) with CD11b^{+} DCs and macrophages in the CIPR database, and may be identified as a unique cluster if a larger starting cell population is used.

The number and strength of cell-cell interactions were highest for myeloid and dedritic cells that suggests a close interaction between monocytes, macrophages, cDC1 and mDC for an effective innate immune response. Consistent with the gene expression profiles, pathway analysis shows suppressed inflammatory (IL-1, TLR) and activated anti-inflammatory/regulatory pathways (RXR, PPAR, vitamin D receptor nuclear receptor signaling) in certain myeloid and DC populations. These findings are consistent with the need to promote immune tolerance and suppress potentially sight threatening inflammation on the ocular surface. We have found RXRα nuclear receptor is expressed by most conjunctival myeloid cells and that the natural ligand 9-cisRA has potent immunosuppressive activity on stimulated monocytes[7,10]. There is increasing recognition that vitamin D signaling through its receptor, a heterodimeric partner of RXR also promotes immune tolerance[34,35].

A surprise finding among the lymphoid cell subsets was that ILC2 had significantly higher expression of the goblet cell trophic factor IL-13 than the other clusters. The physiological importance of IL-13 has been reported to stimulate goblet cell proliferation and mucus production in vivo and in cultured cells[8,9]. The physiological importance of IL-13 on goblet cell maintenance in the conjunctiva is reinforced by reports that antibody neutralization of IL-4Rα, the receptor component shared by IL-4 and IL-13 in patients with atopic dermatitis can cause conjunctival inflammation, dry eye and goblet cell loss[27,36]. We had previously attributed IL-13 production in the conjunctiva to NKT cells; however, it is now recognized that markers used to detect NK cells are also expressed by ILCs[37]. As expected, Il-17 was among the top DEG in γδ T cells. Il-17 has been implicated in the pathogenesis of corneal epithelial barrier disruption and lymphangiogenesis in ocular surface inflammatory disease[16,17,38].

We performed confocal microscopy to immunolocalize cells producing homeostatic and regulatory markers and the findings are summarized in Fig. 5. We found mDC located on the surface of the conjunctiva where they are directly exposed to the environment and pathogens. Both were MHCII[+], and CCR7^{+} mDCs were noted to align with LYVE-1^{+} lymphatic vessels in the superficial stroma. CST3^{+} cDC1 were located within or below the conjunctival epithelium. Monocytes and macrophages were in the stroma below the epithelium and CD209a^{+} macrophages were noted to touch processes of the overlying MHCII^{+} dendritic cells. IL-5/IL-13^{+} ILC2 were located below the conjunctival epithelium and goblet cells where they can provide trophic support for these cells.

There are several shortcomings of this study. This study investigated conjunctival immune cells only in the C57BL/6 strain
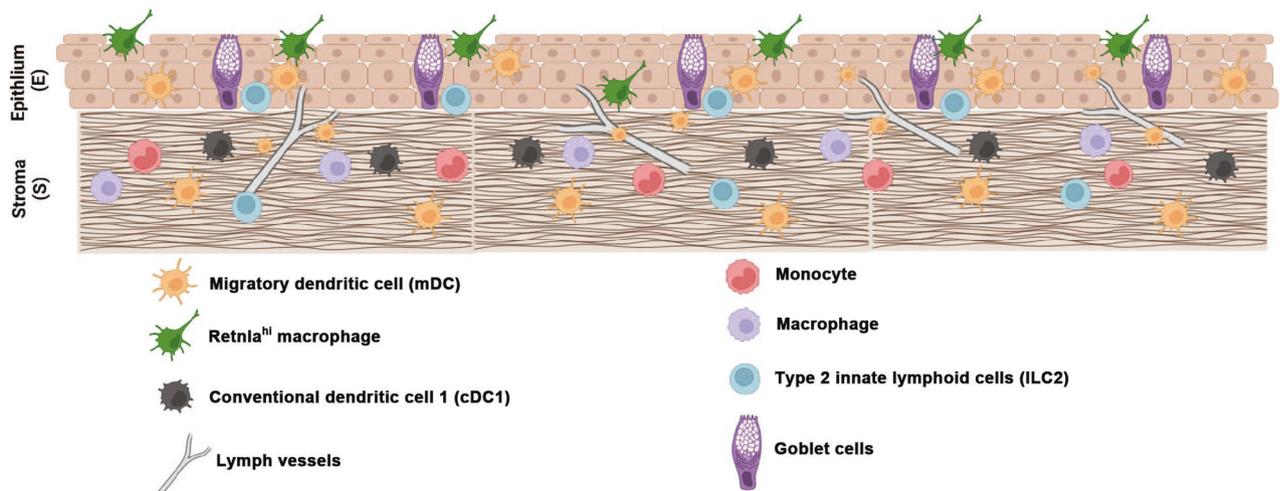

Fig. 5 Schematic showing spacial relationship between conjunctival immune cells with epithelium and stroma. Illustration showing location of immune cells in conjunctival epithelium and stroma.

that was chosen because it is the most frequently used strain for dry eye models, and it is commonly used for studying other infectious and inflammatory diseases, including microbial keratitis. Cluster 0 could be mapped to several cell types, including eosinophils, granulocytes and MHCII[low] macrophages. It wasn't possible to perform immunostaining for highly expressed factors in all cell clusters. Therefore, we concentrated on myeloid cells because they collectively comprised the greatest percentage of cells and because we have previously found that these cells are conditioned by tear and goblet-cell-derived factors[3,39]. We also did not investigate the function of top differentially expressed genes, but these findings provide direction for future studies investigating the role of these genes in conjunctival immunity.

This study provides valuable information that can be used for more specific cell identification and cell-specific gene expression profiles that can be compared with those in ocular surface inflammatory diseases, such as dry eye where there is recruitment and activation of immune cells. It provides biomarkers that can be used to determine factors, such as diet and microbiome, that maintain the production of the homeostatic and regulatory factors by the conjunctival immune cells.

MATERIALS AND METHODS
Animals
The animal protocol for this study was designed according to the ARVO Statement for the use of Animals in Ophthalmic and Vision Research and was approved by the Institutional Animal Care and Use Committee at Baylor College of Medicine (BCM). Female C57BL/6 J (B6) ($n = 8$) mice aged 6–8 weeks were purchased from Jackson Laboratories (Bar Harbor, ME), and allowed to house in a non-stressed (NS) environment at 50–75% relative humidity before the experiment. The age of the mouse at the time of the experiment was 16 weeks.

Flow Cytometry
Conjunctivae were excised, chopped with scissors into tiny pieces, and incubated with 0.1% type IV Collagenase for 1 hour to yield single-cell suspensions. Samples were incubated with anti-CD16/32 (2.4G2, Catalog no. 553141, BD Pharmingen™, San Diego, CA), for 5 minutes at room temperature and subsequently stained with anti-CD45 (clone 30-F11, Catalog no. 103138, BioLegend) and with an infra-red fluorescent viability dye (Catalog no. L10119, Life Technologies, Grand Island, NY). The gating strategy was as follows: lymphocytes were identified by forward -scatter area (FSC-A) and side scatter area (SSC-A) gates, followed by two singlets gates (FSC-A vs. FSC-W and SSC-A vs. SSC-W) followed by live/dead identification using the infra-red fluorescent viability dye. The CD45 + cells were sorted using the Aria-II cell sorter at the Baylor College of Medicine cytometry and cell sorting core.

Library preparation
Single-cell gene expression libraries was prepared using the Chromium Single Cell Gene Expression 3v3.1 kit (×10 Genomics) at the Single Cell Genomics Core at Baylor College of Medicine. In brief, single cells, reverse transcription (RT) reagents, Gel Beads containing barcoded oligonucleotides, and oil were loaded on a Chromium controller (×10 Genomics) to generate single-cell Gel Beads-In-Emulsions (GEMs) where full-length cDNA was synthesized and barcoded for each single cell. Subsequently the GEMs are broken and cDNA from every single cell is pooled. Following cleanup using Dynabeads MyOne Silane Beads, cDNA is amplified by PCR. The amplified product is fragmented to optimal size before end-repair, A-tailing, and adaptor ligation. The final library was generated by amplification.

Sequencing of 10X GEM 3'v3.1 single cell libraries
The BCM Genomic and RNA Profiling (GARP) Core initially conducted sample quality checks using the NanoDrop spectrophotometer and Agilent Bioanalyzer 2100. To quantitate the adapter-ligated library and confirm successful P5 and P7 adapter incorporations, the Applied Biosystems ViiA7 Real-Time PCR System and a KAPA Illumina/Universal Library Quantification Kit (p/n KK4824) was used. The GARP core sequenced the libraries on the NovaSeq 6000

Sequencing System using the S2 v1.0 Flowcell as follows. Cluster Generation by Exclusion Amplification (ExAMP): Using the concentration from the ViiA7 TM qPCR machine above, 150 pM of the equimolar pooled library was loaded onto one lane of the NovaSeq S2 v1.0 flowcell (Illumina p/n 20012,860) following the XP Workflow protocol (Illumina kit p/n 20021,664) and amplified by exclusion amplification onto a nanowell-designed, patterned flowcell using the Illumina NovaSeq 6000 sequencing instrument. PhiX Control v3 adapter-ligated library (Illumina p/n FC-110-3001) was spiked-in at 1% by weight to ensure balanced diversity and to monitor clustering and sequencing performance. The libraries were sequenced according to the 10X Genomics protocol, 28 cycles for Reads 1, 10 cycles each for the i7 and i5 reads, and 90 cycles for Read 2. An average of 251 million read pairs per sample was sequenced. FastQ file generation was executed using bcl2fastq and QC reports were generated using CellRanger v5.0.1 by the BCM Multiomics Core.

Bioinformatic analysis of scRNA-seq data
Raw sequence reads in the FASTQ format were aligned to the mouse reference genome using Cell Ranger Count v6.0.1 pipeline (https://cloud.10xgenomics.com) with the default settings for alignment, barcode assignment, and UMI counting of the raw sequencing data with genome reference Mouse (mm10) 2020-A. The resulting gene expression matrix was subjected to preprocessing following the guideline provided by Seurat v4.1.0.1. Briefly, single cells with fewer than 200 genes and greater than 2500 genes were filtered to remove empty droplets and probable doublets, respectively. We also removed the genes that were expressed in less than 3 cells in our data. In addition, we removed cells that had more than 5% mitochondrial reads. Next, we employ a global-scaling normalization method using the Seurat function "LogNormalize" that normalizes the feature expression.

Clustering, visualization and cell annotation
First, we used the "FindVariableFeatures" function to identify a set of 2500 genes that are highly variable that were used for downstream analysis such as dimensionality reduction and clustering. We then performed Principal Components Analysis (PCA) to construct a linear dimensionality reduction of the dataset that contain most of the complexity of the dataset. The cells were clustered in a graph-based approach within PCA space, and then non-linear dimensionality reductions were applied using UMAP for further visualization purposes. Finally, differential expression was performed using the "FindMarkers" function in Seurat to find cluster-specific marker genes. A heatmap of the top 10 expressing genes of each cluster was prepared. We then used top 20 DEG markers to assign annotation to each cluster using the Cluster Identity Predictor (CIPR) web-based tool (https://aekiz.shinyapps.io/CIPR/).

Cell-cell interaction and gene pathway analysis
Cell-cell interactions were analyzed by CellChat (http://www.cellchat.org/). Gene pathway analysis in each cluster was performed with Qiagen IPA (Germantown, MD).

Whole-mount Immunofluorescence Staining and confocal microscopy
The conjunctival tissue samples were dissected from female C57BL/6 J mice (age 16 weeks) and fixed in 100% methanol for 20 minutes at −20°C followed by washing with Hanks' buffered saline solution (HBSS) for 3 × 5 min with gentle shaking at room temperature (RT). Tissues were permeabilized with 0.4% Triton X-100 in HBSS for 30 minutes at RT and gentle shaking. 20% goat serum (Sigma, USA) diluted in HBSS was used for 1 hour blocking at RT. Subsequently, the conjunctival tissue samples were incubated with primary antibodies (Table S3) diluted in 5% goat serum in HBSS at the mentioned concentrations overnight at 4 °C with gentle shaking at dark. The samples were then washed with 0.4% Triton X-100 for 3 × 6 min at RT with gentle shaking, followed by incubation with secondary antibodies (Supplemental Table 1) diluted in 5% goat serum/HBSS for 1 hour at RT with gentle shaking and light protection. The samples were then washed for 3 × 10 min with 0.4% Triton X-100 in HBSS, and then counterstained with wheat germ agglutinin, Alexa Fluor 647 Conjugate (1:200 in HBSS, ThermoFisher, Cat No. W32466) for visualization of conjunctival goblet cells, and Hoechst (1:500 in HBSS) for nuclei staining (30 min at RT and dark with gentle shaking). The samples were washed 3 × 5 min with HBSS, mounted on slides, and flattened with coverslips. Immunofluorescence staining in whole-mount conjunctival tissue samples was visualized using laser scanning Nikon confocal microscope (Nikon A1 RMP, Nikon, Melville, NY, USA) and 0.5 µm Z-step. The captured images were processed using NIS Elements Advanced Research (AR) software version 4.20 (Nikon).

DATA AVAILABILITY
All raw sequencing data reported have been deposited at this accession URL: https://singlecell.broadinstitute.org/single_cell/study/SCP1614

CODE AVAILABILITY
R scripts used for analysis are available at this Github link: https://github.com/jehanalam82/Cj_B6_CD45_ScRNA-Seq.git

REFERENCES
1. Sacks, E. H., Wieczorek, R., Jakobiec, F. A. & Knowles, D. M II. Lymphocytic subpopulations in the normal human conjunctiva. A monoclonal antibody study. *Ophthalmology* **93**, 1276–1283 (1986).
2. Barabino, S. et al. Immune response in the conjunctival epithelium of patients with dry eye. *Exp. eye Res.* **91**, 524–529 (2010).
3. Ko, B. Y., Xiao, Y., Barbosa, F. L., de Paiva, C. S. & Pflugfelder, S. C. Goblet cell loss abrogates ocular surface immune tolerance. *JCI insight* **3**, e98222 (2018).
4. Zhang, X. et al. NK cells promote Th-17 mediated corneal barrier disruption in dry eye. *PloS one* **7**, e36822 (2012).
5. Alam, J., de Paiva, C. S. & Pflugfelder, S. C. Desiccation induced conjunctival monocyte recruitment and activation - implications for keratoconjunctivitis. *Front Immunol.* **12**, 701415 (2021).
6. Stern, M. E. et al. Autoimmunity at the ocular surface: pathogenesis and regulation. *Mucosal Immunol.* **3**, 425–442 (2010).
7. Alam J., de Paiva C. S. & Pflugfelder S. C. Immune - Goblet cell interaction in the conjunctiva. *Ocul. Surf.* **18**, 326–334 (2020).
8. De Paiva, C. S. et al. Homeostatic control of conjunctival mucosal goblet cells by NKT-derived IL-13. *Mucosal Immunol.* **4**, 397–408 (2011).
9. Henriksson, J. T., Coursey, T. G., Corry, D. B., De Paiva, C. S. & Pflugfelder, S. C. IL-13 stimulates proliferation and expression of mucins and immunomodulatory gene in cultured conjunctival goblet cells. *Investigative Ophthalmol. Vis. Sci.* **56**, 4186–4197 (2015).
10. Alam J., Yu Z., de Paiva C. S. & Pflugfelder S. C. Retinoid regulation of ocular surface innate inflammation. *Int. J. Mol. Sci.* **22**, 1092 (2021).
11. Markoulli, M., Papas, E., Cole, N. & Holden, B. A. The diurnal variation of matrix metalloproteinase-9 and its associated factors in human tears. *Investigative Ophthalmol. Vis. Sci.* **53**, 1479–1484 (2012).
12. An, S. et al. Neutrophil extracellular traps (NETs) contribute to pathological changes of ocular graft-vs.-host disease (oGVHD) dry eye: Implications for novel biomarkers and therapeutic strategies. *Ocul. Surf.* **17**, 589–614 (2019).
13. Bian, F. et al. Differential Effects of Dexamethasone and Doxycycline on Inflammation and MMP Production in Murine Alkali-Burned Corneas Associated with Dry Eye. *Ocul. Surf.* **14**, 242–254 (2016).
14. Grainger, D. J., Reckless, J. & McKilligin, E. Apolipoprotein E modulates clearance of apoptotic bodies in vitro and in vivo, resulting in a systemic proinflammatory state in apolipoprotein E-deficient mice. *J. Immunol. (Baltim., Md: 1950)* **173**, 6366–6375 (2004).
15. Yu, T. et al. Modulation of M2 macrophage polarization by the crosstalk between Stat6 and Trim24. *Nat. Commun.* **10**, 4353 (2019).
16. Sadrai, Z. et al. PDE4 inhibition suppresses IL-17-associated immunity in dry eye disease. *Investigative Ophthalmol. Vis. Sci.* **53**, 3584–3591 (2012).
17. De Paiva, C. S. et al. IL-17 disrupts corneal barrier following desiccating stress. *Mucosal Immunol.* **2**, 243–253 (2009).
18. Jones, L. H. et al. Modulation of dendritic cell alternative activation and function by the vitamin A metabolite retinoic acid. *Int. Immunol.* **27**, 589–596 (2015).
19. Azad A. K., Rajaram M. V. & Schlesinger L. S. Exploitation of the Macrophage Mannose Receptor (CD206) in Infectious Disease Diagnostics and Therapeutics. *J Cytol. Mol. Biol.* **1**, 1000003 (2014).
20. Liu, W. & Spero, D. M. Cysteine protease cathepsin S as a key step in antigen presentation. *Drug N. Perspect.* **17**, 357–363 (2004).
21. Edman, M. C. et al. Increased Cathepsin S activity associated with decreased protease inhibitory capacity contributes to altered tear proteins in Sjögren's Syndrome patients. *Sci. Rep.* **8**, 11044 (2018).
22. Maier, B. et al. A conserved dendritic-cell regulatory program limits antitumour immunity. *Nature* **580**, 257–262 (2020).
23. Rapp, M. et al. CCL22 controls immunity by promoting regulatory T cell communication with dendritic cells in lymph nodes. *J. Exp. Med* **216**, 1170–1181 (2019).
24. Korbecki J. et al. CC Chemokines in a Tumor: A review of pro-cancer and anti-cancer properties of the ligands of receptors CCR1, CCR2, CCR3, and CCR4. *Int. J. Mol. Sci.* **21**,1–9 (2020).
25. Yamashiro, S. Functions of fascin in dendritic cells. *Crit. Rev. Immunol.* **32**, 11–21 (2012).
26. Chabot, V. et al. Unexpected impairment of TNF-α-induced maturation of human dendritic cells in vitro by IL-4. *J. Transl. Med.* **14**, 93 (2016).
27. Utine, C. A., Li, G., Asbell, P., Pflugfelder, S. & Akpek, E. Ocular surface disease associated with dupilumab treatment for atopic diseases. *Ocul. Surf.* **19**, 151–156 (2021).
28. Dohlman, T. H., Ding, J., Dana, R. & Chauhan, S. K. T. Cell-derived granulocyte-macrophage colony-stimulating factor contributes to dry eye disease pathogenesis by promoting cd11b+ myeloid cell maturation and migration. *Investigative Ophthalmol. Vis. Sci.* **58**, 1330–1336 (2017).
29. Collin, J. et al. A single cell atlas of human cornea that defines its development, limbal progenitor cells and their interactions with the immune cells. *Ocul. Surf.* **21**, 279–298 (2021).
30. Laskowitz, D. T. et al. Downregulation of microglial activation by apolipoprotein E and apoE-mimetic peptides. *Exp. Neurol.* **167**, 74–85 (2001).
31. Conde, P. et al. DC-SIGN(+) Macrophages Control the Induction of Transplantation Tolerance. *Immunity* **42**, 1143–1158 (2015).
32. Ahadome S. D. et al. Classical dendritic cells mediate fibrosis directly via the retinoic acid pathway in severe eye allergy. *JCI Insight* **1**, e87012 (2016)
33. Bosteels, C. et al. Inflammatory type 2 cDCs acquire Features of cDC1s and macrophages to orchestrate immunity to respiratory virus infection. *Immunity* **52**, 1039–1056 (2020).
34. Badenhoop, K., Kahles, H. & Penna-Martinez, M. Vitamin D, immune tolerance, and prevention of type 1 diabetes. *Curr. Diab Rep.* **12**, 635–642 (2012).
35. Roszer, T., Menendez-Gutierrez, M. P., Cedenilla, M. & Ricote, M. Retinoid X receptors in macrophage biology. *Trends Endocrinol. Metab.* **24**, 460–468 (2013).
36. Bakker D. S. et al. Goblet cell scarcity and conjunctival inflammation during treatment with dupilumab in patients with atopic dermatitis. *British J. Dermatol.* **180**, 1248–1249 (2019).
37. Galletti, J. G. & de Paiva, C. S. The ocular surface immune system through the eyes of aging. *Ocul. Surf.* **20**, 139–162 (2021).
38. Chauhan, S. K. et al. A novel pro-lymphangiogenic function for Th17/IL-17. *Blood* **118**, 4630–4634 (2011).
39. Xiao, Y. et al. Goblet cell produced retinoic acid suppresses CD86 expression and IL-12 production in bone marrow derived cells. *Int Immunol.* **25**, 457–470 (2018).

AUTHOR CONTRIBUTIONS
S.C.P., J.A. and R.R.P. were involved in conception and design of the study. J.A., S.C.P. and G.Y. were involved in data acquisition. J.A., S.C.P., R.R.P., N.B., G.Y. and C.S.D.P. were involved in data analysis and interpretation. S.C.P., J.A., R.P. and G.Y. drafted the manuscript. All authors revised the manuscript critically for important intellectual content and approved the submitted version.

COMPETING INTERESTS
The authors declare no competing interests.

ADDITIONAL INFORMATION
Supplementary information The online version contains supplementary material available at https://doi.org/10.1038/s41385-022-00507-w.

Correspondence and requests for materials should be addressed to Stephen C. Pflugfelder.

Reprints and permission information is available at http://www.nature.com/reprints

Publisher's note Springer Nature remains neutral with regard to jurisdictional claims in published maps and institutional affiliations.